European Review for Medical and Pharmacological Sciences 2013; 17: 2902-2908

Dexamethasone inhibits the effect of paclitaxel on human ovarian carcinoma xenografts in nude mice

W.J. HOU, J.H. GUAN, Q. DONG, Y.H. HAN, R. ZHANG

Department of Obstetrics and Gynecology, Shanghai Jiaotong University-Affiliated Sixth People's Hospital of Fengxian Branch, Shanghai, China

Abstract. – BACKGROUND: Recent studies showed that dexamethasone (DEX) could render cancer cells resistant to paclitaxel (PTX) induced apoptosis though an unknown mechanism.

AIM: This study aimed to evaluate the influence of DEX pretreatment on the anti-tumor effect of PTX in an *in vivo* xenograft model with grafted ovarian cancer SKOV-3 cells innude mice.

MATERIALS AND METHODS: The xenograft procedure was performed, and the nude mice were grouped into four cohorts of ten that received the following treatments: Control group, DEX group, PTX group and DEX+PTX group. Individual treatments were administered once every three days for a total of 6 courses. The growth of tumors and the inhibition rates were measured. Changes in tissue morphology and cellular ultrastructure were observed using light and transmission electron microscopy. Immunohistochemistry was performed to examine the expression of Ki-67, Bcl-xL and cleaved caspase-3.

RESULTS: Premedication with DEX reduced the inhibitory effect of PTX on tumor growth by approximately 20% compared to the PTX-only-treated group in the ovarian carcinoma xenografted mice. Hematoxylin-eosin (H&E) staining revealed that significantly fewer cells exhibited vacuolization and apoptosis in the DEX + PTX group compared to the PTX group. Apoptotic characteristics including karyopyknosis, nuclear chromatin condensation along the nuclear membrane and aggregation were observed in both DEX+PTX and PTX groups under electron microscopy. However, these characteristics were less significant in the DEX+PTX group than those in the PTX group. The immunohistochemistry demonstrated that protein expression levels of Ki-67 and Bcl-xL were significantly increased, whereas cleaved caspase-3 decreased in the DEX+PTX group, compared to PTX group ($p < 0.0125$).

CONCLUSIONS: DEX inhibits the therapeutic efficacy of PTX in a human ovarian carcinoma SKOV-3 xenograft model.

Key Words:
Dexamethasone, Paclitaxel, Ovarian carcinoma, Apoptosis, Bcl-xL, Cleaved Caspase-3.

Introduction

Paclitaxel (PTX) is a natural antitumor agent with significantly therapeutic effect against solid tumors, particularly for advanced inoperable ovarian cancer and metastatic ovarian cancer after failure of first-line or multiple chemotherapies[1-4]. However, the use of PTX may produce severe or lethal side effects such as hypersensitivity[5-6]. Thus, dexamethasone (DEX) is routinely used as a premedication in the clinical application of paclitaxel to prevent hypersensitivity reactions. Interestingly, recent studies have shown that DEX could render cancer cells resistant to PTX induced apoptosis, though the underlying mechanisms are largely unknown[7-9]. Thus, it is of great clinical interest to investigate whether DEX interferes with the therapeutic efficacy of PTX via the inhibition of PTX-induced apoptosis in human ovarian cancer. The present study used an *in vivo* model, of which human ovarian carcinoma SKOV-3 cells were xenografted into nude mice, to determine the effects and possible mechanisms of DEX on the antitumor efficacy of PTX. The obtained results have potential implications to properly applying DEX and the developing new routes of PTX administration in clinical practices.

Materials and Methods

Cell Culture

Human ovarian serous adenocarcinoma cell line, SKOV-3 was kindly provided by Dr. Xiu-Li Shang (Department of Neurophysiology, Affiliated First Hospital, China Medical University, China). The SKOV-3 cell line was routinely maintained in Rosswell Park Memorial Institute (RPMI) 1640 medium (Gibco, Grand Island, NY, USA) supplemented with 10% hormone-stripped fetal calf serum (FCS) (the Center of Biotechnology, Fudan University, China). The cells were grown at 37°C in a humidified atmosphere of 5% CO_2 and were passed every 2-3 days.

Corresponding Author: Rong Zhang, MM; e-mail: ronggzhang@hotmail.com

Inoculation of Tumor Cells

All animal studies have been approved by China Ethics Committee and performed in accordance with the ethical standards. BALB/c (nu/nu) mice (female, age: 4-8 weeks, weight: 18-22 g) were purchased from the Shanghai Laboratory Animal Center, the Chinese Academy of Sciences [Certificate number: SCXK (Shanghai) 2003-0003]. The mice were bred in a specific pathogen-free (SPF) environment at the Animal Laboratory in Shanghai Laboratory Animal Center, Chinese Academy Science [approval number: SYXK (Shanghai) 2004-0011].

SKOV-3 cells in a logarithmic growth phase were collected by standard trypsin digestion. Viable cells were quantified to adjust the total cell concentration to be $1\text{-}3\times10^7$/ml. Mouse skin was disinfected at the point of injection. A total volume of 100-200 mL of the cell suspension was injected subcutaneously in the right flank of the intercostal space in each mouse.

Collection and Inoculation of Tumor Tissue

The nude mice were sacrificed using cervical translocation when a successfully inoculated primary tumor reached 0.8-1.0 cm in diameter. The subcutaneous tumor was harvested and cut into slices with a diameter of 1-2 mm. A 12-gauge syringe was used to collect the small tumor specimens, which were then subcutaneously inoculated into a new nude mouse. This inoculation procedure was completed within 30 min after the harvesting of the primary tumor from the body.

In vivo Treatment of DEX and PTX

The nude mice were randomly divided into four groups of ten animals each when the average diameter of the tumors reached 6-7 mm in 8-10 days after tumor formation: (1) control group; (2) DEX group: 1 mg/kg DEX (Sigma Chemical Co., St Louis, MO, USA) intraperitoneally; (3) PTX group: 20 mg/kg PTX (Bristol-Myers Squibb Co., New York, NY, USA) intravenously; (4) DEX+PTX group: 1 mg/kg DEX (ip) followed by 20 mg/kg PTX (iv) after 12 hours. Individual treatments were administered once every three days for a total of 6 courses.

Evaluation of Xenografts in Nude Mice

The largest (a) and smallest diameters (b) of the xenografts were measured using calipers on the day after treatment administration during the entire treatment period. The xenograft volume (v) was calculated according to the formula: $V = \pi\times ab^2/6$. The evaluation of treatment efficacy was based on comparisons between the experimental and the control groups. The tumor growth curve was plotted after treatment using the tumor volumes from the indicated times. The animals were sacrificed after treatment, and the tumors were harvested and weighed. The inhibition rates (IR) of tumor growth were calculated according to the following formula: IR = (average tumor weight of control group – average tumor weight of treatment group)/average tumor weight of control group$\times100\%$[10].

Histopathological Analysis of Xenografts

The subcutaneous xenografts were obtained from the nude mice and fixed in 10% neutral formalin. The xenografts were then embedded in paraffin wax, sectioned and stained using hematoxylin-eosin (H&E). Histological studies were performed under a light microscope.

Quantification of Protein Expression Using Semi-Quantitative Immuno-Histochemical Analysis

Two-step visualization systems from DakoEnVision™ were applied. The primary antibody was substituted with phosphate-buffered solution (PBS) in the negative controls. The positive controls were histological sections of ovarian carcinoma with known expressions of Ki-67, Bcl-xL and cleaved caspase-3. Semi-quantitative analysis was performed according to the scoring standard described previously[11]. Ten high-power fields (400 magnifications) from each slide were randomly selected and examined under a light microscope. The scoring was performed according to staining intensity (i.e., score 0 = no stain; score 1 = light stain; score 2 = medium stain; and score 3 = dark stain) and the percentage of positively stained cells (i.e., score 0 = no stain; score 1 = smaller than 25 % cells; score 2 = 25-50 % cells; score 3 = more than 50 % cells). The scores of staining intensity and the percentage of positively stained cells were summed, and the following score ranges were defined, as a summation score of 0-2 indicating negative expression (-), a summation score > 2 positive expression, a summation score of 3-4 weak positive expression (+) and a summation score of 5-6 strong positive expression (++). Ki-67 expression was localized to the nuclei as light brownish-yellow granules, while Bcl-xL and cleaved caspase-3 expression were localized in the cytoplasm, cell membranes and brownish-yellow granules.

Statistical Analysis

All of the data in this study were analyzed using the statistical software, SAS8.2 and are presented means ± standard deviations. Comparisons between multiple groups were performed using an analysis of variance (ANOVA) followed by the least significant difference *t* (LSD-*t*) test for multiple means comparisons. $p < 0.05$ was considered statistically significant. Non-parametric statistics were applied when appropriate. A non-parametric process model was used for further comparisons in case there are statistically significant differences between the four groups ($\alpha = 0.00714$).

Results

Effect of DEX on Tumor Growth Inhibition Induced by PTX in SKOV-3 Xenografts in Nude Mice

Changes in the Volume of SKOV-3 Xenografts in Nude Mice

The largest (a) and smallest diameters (b) of the SKOV-3 xenografts were measured using calipers on the day after treatment administration during the entire treatment period. The xenograft volume (V) was calculated according to the formula: $V = \pi \times ab^2/6$. The changes in volume over time in each group are presented in Figure 1. The volumes of the tumors from the PTX and DEX+PTX groups were significantly smaller than the volume of tumor in control group ($p < 0.01$). Moreover, the volumes of the tumors from the PTX group were significantly smaller than the one of DEX+PTX group ($p < 0.05$).

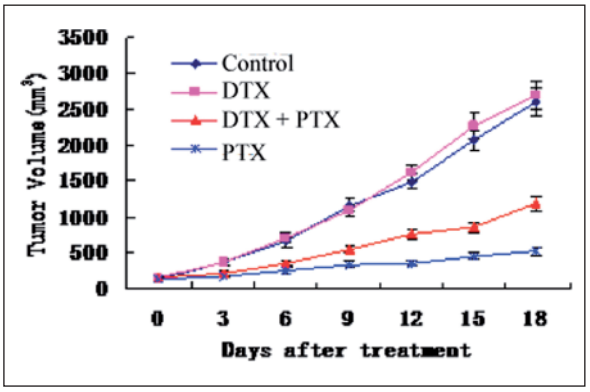

Figure 1. The effects of various treatments on the volumes of xenografts in nude mice. Xenograft volumes in the control and DEX treated groups were highest, and the volume of tumor in DEX+PTX group was smaller, compared to PTX-treated group, which had the smallest volume of xenografts.

Changes in Tumor Weight and Tumor Growth Rate Inhibition of SKOV-3 Xenografts in Nude Mice

The different treatment groups exhibited the following tumor weights: 1.43±0.13 g for the control group; 1.53±0.16 g for the DEX group; 0.79±0.09 g for the DEX+PTX group; and 0.52±0.06 g for the PTX group. The differences between the control group and the DEX+PTX and PTX groups were significant ($p < 0.01$). The tumor growth inhibition rates of the DEX+PTX and PTX groups were 44.76% and 63.64%, respectively, and the rate of DET+PTX group was 18-25 % smaller than the rate of PTX group ($p < 0.01$). Our results demonstrated that pretreatment with DEXsignificantly attenuated the therapeutic efficacy of PTX.

Histological and Morphological Examination of DEX-mediated Suppression on the PTX-induced Effect on SKOV-3 Xenografts in Nude Mice

Most of the cells in the PTX group were enlarged and exhibited significantly less cytoplasm (typical characteristics of apoptosis) compared to the other groups. The DEX+PTX group exhibited significantly fewer tumor cells with vacuolization or apoptosis, compared to the PTX group (Figure 2).

Alterations in Cellular Ultrastructure Under Electron Microscopy

The majority of the cells in the DEX and control groups exhibited clear cell membrane, cell volume and normal morphology. The nuclei were located in the center of the cells with regular morphologies (i.e., oval shape). The border of the nuclear membrane was clear. Chromatin was distributed equally in the nuclei. The nucleoli were evident and of adequate sizes (Figure 3). Most cells in the PTX group exhibited a clear cell membrane with karyopyknosis and irregular morphologies, heterochromatin condensation, condensed chromatin adjacent to the nuclear membrane and aggregation, cell atrophy or partial collapse phenomena. These features are typical characteristics of apoptosis at various stages. These characteristics were also observed in the DEX+PTX group. However, apoptotic cells in the DEX+PTX group were less frequent compared to PTX group.

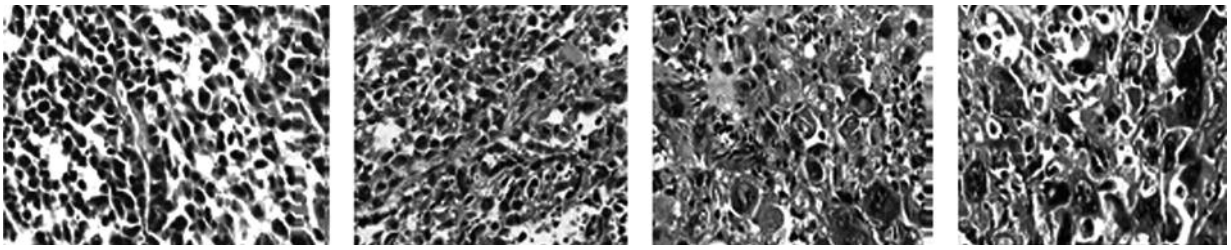

Figure 2. H&E staining of tumor sections with different treatments. **A**, Control group; **B**, DEX group; **C**, DEX+PTX group; **D**, PTX group. Most cells in the PTX group were enlarged and exhibited significantly less cytoplasm than the cells inother groups. Tumor cells exhibited vacuolization and apoptosis in the DEX+PTX group, but the degree was less significant compared to the PTX group (200 magnifications).

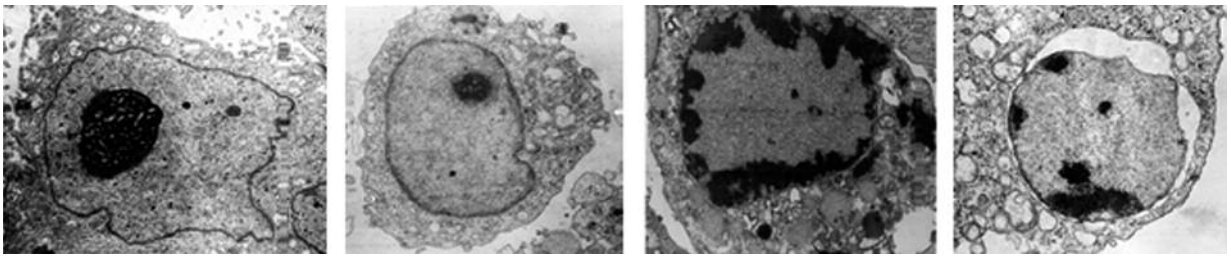

Figure 3. Alterations in cellular ultrastructure under transmission electron microscopy (X 10,000). **A**, Normal cells; **B**, early-stage apoptotic cells; **C**, mid-stage apoptotic cells; and (**D**) late-stage apoptotic cells.

Effects of DEXon the Cell Proliferative Marker Ki-67

We used immunohistochemistry to analyze the cell proliferative marker Ki-67. No significant differences in the expression of Ki-67 were observed between the DEX and control groups ($p > 0.05$). The expressions of Ki-67 in both treatment groups (DEX+PTX and PTX) were significantly lower than that in the control group ($p < 0.0125$). The tumor cells in the DEX+PTX group exhibited higher expression levels of Ki-67, compared to PTX group ($p < 0.0125$) (Table I). Using a conventional light microscope, Ki-67 expression was clearly observed to be localized in nuclei as light brownish-yellow granules (Figure 4A).

Effect of DEXon the Protein Expression of Bcl-xL and Cleaved Caspase-3

No significant differences in Bcl-xL and cleaved caspase-3 protein expression were observed between the control and DEX groups ($p > 0.05$). However, significant differences were observed between the DEX+PTX and PTX groups ($p < 0.0001$). Tumor cells in the DEX+PTX group demonstrated higher expression levels of Bcl-xL protein but lower expression of levels of cleaved caspase-3, compared to the PTX group ($p < 0.0001$) (Table I). The expression of Bcl-xL and cleaved caspase-3 were observed in the cytoplasm and cell membranes as light brownish-yellow granules under a conventional light microscope (Figure 4B and C).

Discussion

There have been notable changes in first-line chemotherapy against ovarian cancer, including the use of paclitaxel. Study by the American Gynecologic Oncology Group (GOG) demonstrates that combination therapy with taxol and cisplatin exhibits superior efficacy vs. the traditional regimen of cisplatin and cyclophosphamide and reduces the recurrence and mortality rates of ovarian cancer by 28% and 34%, respectively. The results from the International Collaborative Ovarian Neoplasm trial (lCON) also reveale that combined chemotherapy with taxol and cisplatin reduces the recurrence rate of ovarian cancer by 34%[12]. Therefore, combined chemotherapy with taxol and cisplatin is the first choice for first-line chemotherapy in ovarian cancer. Unfortunately, hypersensitivity reactions are potential adverse effects of PTX[7,13]. Minor hypersensitivity reactions are characterized by a redness of the face, skin rashes and body formication, and severe hypersensitivity reactions are characterized by hy-

Table I. Expression of Ki-67, Bcl-xL, and cleaved caspase-3 protein in four groups.

Markers	Groups	View	Expression			X^2	*p*-value
			–	+	++		
Ki-67	Control	100	16	61	23		
	DEX	100	18	57	25	0.0180*	0.9856
	PTX	100	90	7	3	10.0160*#	< 0.0001
	DEX+PTX	100	63	20	17	5.4178*#	< 0.0001
Bcl-xL	Control	100	23	50	27		
	DEX	100	25	47	28	0.0083*	0.9272
	DEX+PTX	100	68	21	11	35.6494*	< 0.0001
	PTX	100	87	9	4	77.0391*#	< 0.0001
Cleaved caspase-3	Control	100	77	15	8		
	DEX	100	73	20	7	0.3104*	0.5774
	DEX + PTX	100	57	27	16	8.8836*	0.0029
	PTX	100	31	48	21	37.9111*#	< 0.0001

*Compared with the control group, #compared with the DEX + PTX group.

potension, bradycardia, bronchospasm and anaphylactic shock, which may lead to death[14-17]. DEX (20 mg) is routinely administered orally as a premedication 6 and 12 hours before the clinical application of PTX to prevent the appearance of hypersensitivity. However, recent studies have suggested that DEX selectively inhibits chemotherapy-induced apoptosis in tumor cells.

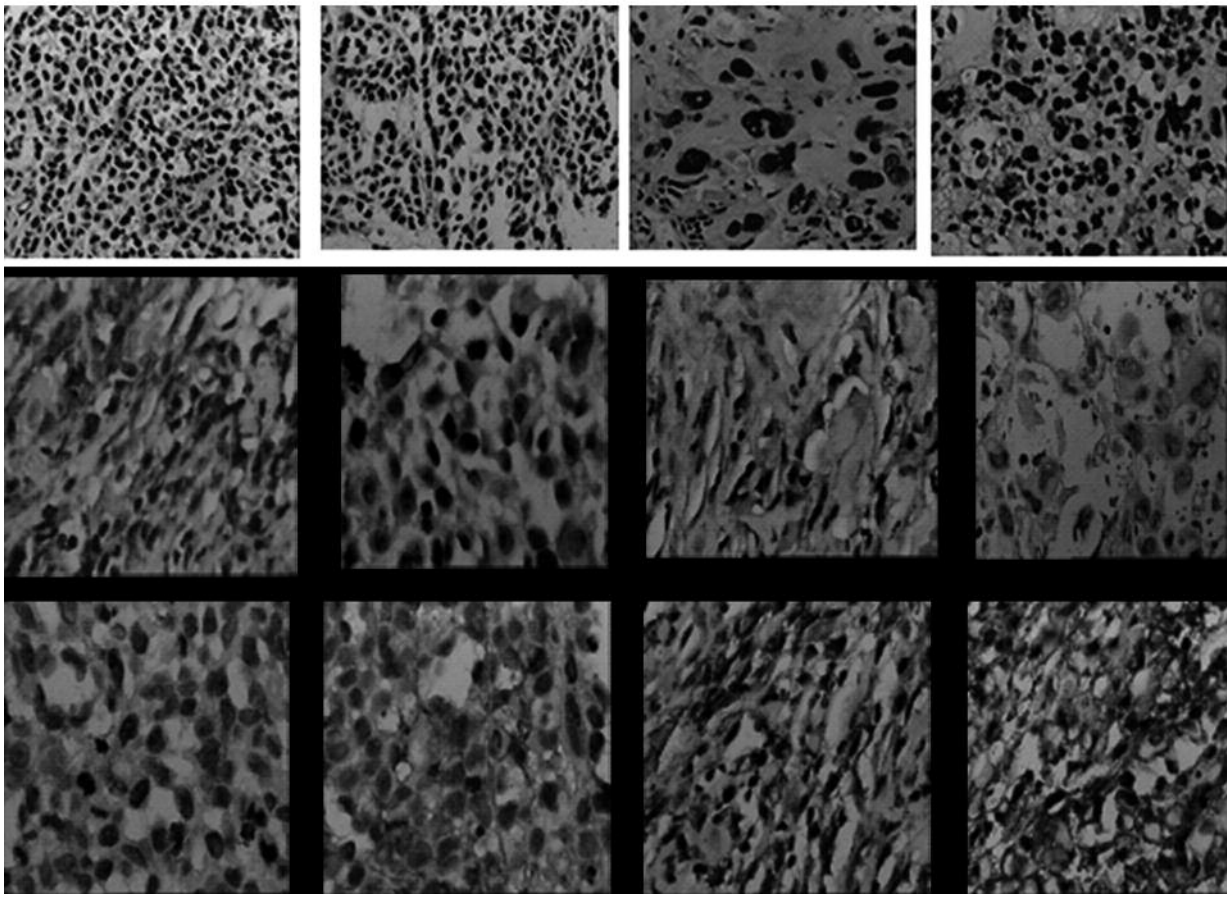

Figure 4. Immunohistochemical staining of cell proliferative marker Ki-67, Bcl-xL protein and cleaved caspase-3 protein in SKOV-3 xenografts in nude mice with the different treatment groups.

Thus, whether pretreatment with DEX interferes with the therapeutic efficacy of PTX through the inhibition of PTX-induced apoptosis in tumor cells is of great interest in clinical research. To gain an insight of the possible mechanisms, we established an *in vivo* nude mice model bearing ovarian carcinoma xenografts to study the differences between the PTX-treatment (20 mg/kg intravenous injection) and pretreatment of DEX (1 mg/kg peritoneal injection 12 hours before PTX, which is close to the clinical dosage). Our findings showed that tumor growth inhibition rates were 44.76% and 63.64% with the treatments of DEX+PTX and PTX, compared to control condition, respectively. The tumor growth inhibition rate in the PTX group was 18-25% higher than the rate in the DEX+PTX group ($p < 0.01$). Therefore, pretreatment with DEX significantly reduced the anti-tumor effect of PTX on ovarian carcinoma xenografts in nude mice.

The inhibitory effect of DEX on PTX -induced apoptosis was accidentally discovered in an estrogen/androgen-induced leiomyosarcoma cell line (DDT1 MF2) in which the cell-killing activity of PTX is significantly reduced by DEX pretreatment[18]. The inhibitory effect of DEX on PTX may not relate to cell cycle control because glucocorticoids have no impact on PTX-mediated arrest of mitosis or cell cycle[19]. Several lines of evidences have shown that the inhibitory effect of DEX on the therapeutic activity of PTX seems to be apoptosis-specific because PTX-mediated mitotic arrest or cell cycle distribution is unaffected or marginally affected by the steroid[20-22].

It is well known that caspase-3 is the effector caspase in apoptosis and can be activated by irradiation, chemotherapeutics, or members of the tumor necrosis factor family[23-26]. Therefore, DEX may reduce the PTX-induced expression of key elements of the cell death receptor pathway, such as cleaved caspase-3, in ovarian cancer. We analyzed the activities of the antiapoptotic protein, Bcl-xL and cysteine protease caspase-3, downstream factors in the apoptotic pathway, to characterize the mechanisms of the inhibitory effect of DEX on PTX-induced apoptosis. The results demonstrated that pretreatment with DEX upregulated the expression of Bcl-xL but down-regulated the activity of caspase-3. This result suggested that DEX inhibited PTX-induced apoptosis in SKOV-3 cells via the induction of Bcl-xL expression and reduction in caspase-3 activity.

Conclusions

We demonstrated that pretreatment with DEX significantly inhibited the therapeutic efficacy of PTX in our nude mouse model bearing a human ovarian carcinoma xenograft. Though the exact mechanism of the antagonistic effect of DEX on the activity of paclitaxel is not clear, our findings demonstrated that dexamethasone interfered with the medical effect of PTX and inhibited PTX-induced apoptosis. These results may advance our understanding of the proper clinical use of dexamethasone. Novel routes of administration for PTX may be developed for future clinical practice to prevent adverse effects without reducing the therapeutic efficacy of PTX.

Conflict of Interest

The Authors declare that there are no conflicts of interest.

References

1) Wu R, Baker SJ, Hu TC, Norman KM, Fearon ER, Cho KR. Type I to Type II ovarian carcinoma progression: mutant Trp53 or Pik3ca confers a more aggressive tumor phenotype in a mouse model of ovarian cancer. Am J Pathol 2013; 182: 1391-1399.

2) Kawaguchi R, Tanase Y, Haruta S, Nagai A, Yoshida S, Furukawa N, Ooi H, Kobayashi K. Paclitaxel plus carboplatin chemotherapy for primary peritoneal carcinoma: a study of 22 cases and comparison with stage III, IV ovarian serous carcinoma. Case Rep Oncol 2012; 5: 173-180.

3) Hatziveis K, Tourlakis D, Hountis P, Kyriazanos I, Sougleri M, Ginopoulos P, Camoutsis C. Effects on the immune system and toxicity of carboplatin/paclitaxel combination chemotherapy in patients with stage III-IV ovarian and non small cell lung cancer and its role in survival and toxicity. J BUON 2012; 17: 143.

4) Hoskins P, Vergote I, Cervantes A, Tu D, Stuart G, Zola P, Poveda A, Provencher D, Katsaros D, Ojeda B, Ghatage P, Grimshaw R, Casado A, Elit L, Mendiola C, Sugimoto A, D'Hondt V, Oza A, Germa JR, Roy M, Brotto L, Chen D, Eisenhauer EA. Advanced ovarian cancer: phase III randomized study of sequential cisplatin-topotecan and carboplatin-paclitaxel vs carboplatin-paclitaxel. J Natl Cancer Inst 2010; 102: 1547-1556.

5) Zhang C, Qu G, Sun Y, Wu X, Yao Z, Guo Q, Ding Q, Yuan S, Shen Z, Ping Q, Zhou H. Pharmacokinetics, biodistribution, efficacy and safety of N-octyl-O-sulfate chitosan micelles loaded with paclitaxel. Biomaterials 2008; 29: 1233-1241.

6) Liu K, Cang S, Ma Y, Chiao JW. Synergistic effect of paclitaxel and epigenetic agent phenethyl isothio-

cyanate on growth inhibition, cell cycle arrest and apoptosis in breast cancer cells. Cancer Cell Int 2013; 13: 10.

7) Gruver-Yates AL, Cidlowski JA. Tissue-specific actions of glucocorticoids on apoptosis: a Double-Edged Sword. Cells 2013; 2: 202-223.

8) Vogt A, McDonald PR, Tamewitz A, Sikorski RP, Wipf P, Skoko JJ 3rd, Lazo JS. A cell-active inhibitor of mitogen-activated protein kinase phosphatases restores paclitaxel-induced apoptosis in dexamethasone-protected cancer cells. Mol Cancer Ther 2008; 7: 330-340.

9) Pang D, Kocherginsky M, Krausz T, Kim SY, Conzen SD. Dexamethasone decreases xenograft response to Paclitaxel through inhibition of tumor cell apoptosis. Cancer Biol Ther 2006; 5: 933-940.

10) Zhu X, Sui M, Fan W. In vitro and in vivo characterizations of tetrandrine on the reversal of P-glycoprotein-mediated drug resistance to paclitaxel. Anticancer Res 2005; 25: 1953-1962.

11) Vakkala M, Kahlos K, Lakari E, Paakko P, Kinnula V, Soini Y. Inducible nitric oxide synthase expression, apoptosis, and angiogenesis in situ and invasive breast carcinomas. Clin Cancer Res 2000; 6: 2408-2416.

12) Parmar MK, Ledermann JA, Colombo N, du Bois A, Delaloye JF, Kristensen GB, Wheeler S, Swart AM, Qian W, Torri V, Floriani I, Jayson G, Lamont A, Tropé C. Paclitaxel plus platinum-based chemotherapy versus conventional platinum-based chemotherapy in women with relapsed ovarian cancer: the ICON4/AGO-OVAR-2.2 trial. Lancet 2003; 361: 2099-2106.

13) Iwamoto T. Clinical application of drug delivery systems in cancer chemotherapy: review of the efficacy and side effects of approved drugs. Biol Pharm Bull 2013; 36: 715-718.

14) Mayerhofer K, Bodner-Adler B, Bodner K, Leodolter S, Kainz C. Paclitaxel/carboplatin as first-line chemotherapy in advanced ovarian cancer: efficacy and adverse effects with special consideration of peripheral neurotoxicity. Anticancer Res 2000; 20: 4047-4050.

15) Kumagai M, Fujii T, Komatsu M, Kusuda T, Takehara K, Shinkou S, Naitou H. [Paclitaxel plus carboplatin in ovarian cancer-comparison of adverse effects between monthly and weekly administration]. Gan To Kagaku Ryoho 2004; 31: 555-559.

16) Bergmann TK, Gréen H, Brasch-Andersen C, Mirza MR, Herrstedt J, Hølund B, du Bois A, Damkier P, Vach W, Brosen K, Peterson C. Retrospective study of the impact of pharmacogenetic variants on paclitaxel toxicity and survival in patients with ovarian cancer. Eur J Clin Pharmacol 2011; 67: 693-700.

17) Konishi Y, Sato H, Sato N, Fujimoto T, Fukuda J, Tanaka T. Scleroderma-like cutaneous lesions induced by paclitaxel and carboplatin for ovarian carcinoma, not a single course of carboplatin, but re-induced and worsened by previously administrated paclitaxel. J Obstet Gynaecol Res 2010; 36: 693-696.

18) Sui M, Chen F, Chen Z, Fan W. Glucocorticoids interfere with therapeutic efficacy of paclitaxel against human breast and ovarian xenograft tumors. Int J Cancer 2006; 119: 712-717.

19) Fan W, Sui M, Huang Y. Glucocorticoids selectively inhibit paclitaxel-induced apoptosis: mechanisms and its clinical impact. Curr Med Chem 2004; 11: 403-411.

20) Chen YX, Wang Y, Fu CC, Diao F, Song LN, Li ZB, Yang R, Lu J. Dexamethasone enhances cell resistance to chemotherapy by increasing adhesion to extracellular matrix in human ovarian cancer cells. Endocr Relat Cancer 2010; 17: 39-50.

21) Huang Y, Fan W. IkappaB kinase activation is involved in regulation of paclitaxel-induced apoptosis in human tumor cell lines. Mol Pharmacol 2002; 61: 105-113.

22) Huang Y, Fang Y, Dziadyk JM, Norris JS, Fan W. The possible correlation between activation of NF-kappaB/IkappaB pathway and the susceptibility of tumor cells to paclitaxel-induced apoptosis. Oncol Res 2002; 13: 113-122.

23) Galon J, Franchimont D, Hiroi N, Frey G, Boettner A, Ehrhart-Bornstein M, O'Shea JJ, Chrousos GP, Bornstein SR. Gene profiling reveals unknown enhancing and suppressive actions of glucocorticoids on immune cells. FASEB J 2002; 16: 61-71.

24) Igney FH, Krammer PH. Death and anti-death: tumour resistance to apoptosis. Nat Rev Cancer 2002; 2: 277-288.

25) Kaufmann SH, Hengartner MO. Programmed cell death: alive and well in the new millennium. Trends Cell Biol 2001; 11: 526-534.

26) Ashkenazi A. Targeting death and decoy receptors of the tumour-necrosis factor superfamily. Nat Rev Cancer 2002; 2: 420-430.